0026-895X/11/8002-328–336$25.00
MOLECULAR PHARMACOLOGY
Copyright © 2011 The American Society for Pharmacology and Experimental Therapeutics
Mol Pharmacol 80:328–336, 2011

Vol. 80, No. 2
71985/3704548
Printed in U.S.A.

Site-Directed Mutagenesis of the CC Chemokine Binding Protein 35K-Fc Reveals Residues Essential for Activity and Mutations That Increase the Potency of CC Chemokine Blockade[S]

Gemma E. White, Eileen McNeill, Ivy Christou, Keith M. Channon, and David R. Greaves

Sir William Dunn School of Pathology (G.E.W., I.C., D.R.G.) and Department of Cardiovascular Medicine (E.M., K.M.C.), University of Oxford, Oxford, United Kingdom

Received February 25, 2011; accepted May 17, 2011

ABSTRACT

Chemokines of the CC class are key mediators of monocyte recruitment and macrophage differentiation and have a well documented role in many inflammatory diseases. Blockade of chemokine activity is therefore an attractive target for anti-inflammatory therapy. 35K (vCCI) is a high-affinity chemokine binding protein expressed by poxviruses, which binds all human and murine CC chemokines, preventing their interaction with chemokine receptors. We developed an Fc-fusion protein of 35K with a modified human IgG1 Fc domain and expressed this construct in human embryonic kidney 293T cells. Purified 35K-Fc is capable of inhibiting CC chemokine-induced calcium flux, chemotaxis, and β-arrestin recruitment in primary macrophages and transfected cells. To elucidate the residues involved in chemokine neutralization, we performed site-directed mutagenesis of six key amino acids in 35K and expressed the mutant Fc-fusion proteins in vitro. We screened the mutants for their ability to block chemokine-induced β-arrestin recruitment in transfected cells and to inhibit primary macrophage signaling in an electric cell substrate impedance sensing assay. Using a sterile model of acute inflammation, zymosan-induced peritonitis, we confirmed that wild-type 35K-Fc can reduce monocyte recruitment, whereas one mutant (R89A) showed a more pronounced blockade of monocyte influx and another mutant (E143K) showed total loss of function. We believe that 35K-Fc will be a useful tool for exploring the role of CC chemokines in chronic inflammatory pathologies, and we have identified a higher potency form of the molecule that may have potential therapeutic applications in chronic inflammatory disease.

Introduction

Fc fusion proteins and monoclonal antibodies that block the activity of circulating inflammatory mediators are now an essential arm of therapies directed against chronic inflammatory pathologies such as rheumatoid arthritis (Taylor and Feldmann, 2009). One of the most successful drugs in this class is the TNFR:Fc fusion protein etanercept (Enbrel; Immunex Corporation, Thousand Oaks, CA), a fusion of TNFR2 with a human IgG1 Fc domain that functions as a decoy receptor for soluble TNFα (Moreland et al., 1997). The addition of an Fc domain greatly increases the half-life of the TNFR protein in plasma, such that dosing is reduced to once or twice weekly injections (Moreland et al., 1996). A wide range of other soluble mediators could be targeted with this approach, because not all patients respond to anti-TNF therapy and the efficacy of treatment may decrease over time, meaning novel targets are required (Taylor and Feldmann, 2009). One candidate class of soluble inflammatory mediators is the chemokines or chemotactic cytokines, the low-molecular-weight proteins responsible for the coordinated migration of leukocytes in response to inflammation and infection (Mackay, 2001; Charo and Ransohoff, 2006).

Most viruses express a repertoire of proteins, including chemokine binding proteins, which interfere with the host immune response as a means to avoid rapid elimination from the organism (Alcami, 2003). Chemokines are divided into

This work was funded by the British Heart Foundation [Grant RG/05/011].
Article, publication date, and citation information can be found at http://molpharm.aspetjournals.org.
doi:10.1124/mol.111.071985.
[S] The online version of this article (available at http://molpharm.aspetjournals.org) contains supplemental material.

ABBREVIATIONS: TNF, tumor necrosis factor; ECIS, electric cell-substrate impedance sensing; MR, mannose receptor; LTB4, leukotriene B4; MCP-1, monocyte chemotactic protein-1; MIP, macrophage inflammatory protein; RANTES, regulated upon activation, normal T-cell expressed, and secreted; PCR, polymerase chain reaction; BSA, bovine serum albumin; PBS, phosphate-buffered saline; CHO, Chinese hamster ovary; ELISA, enzyme-linked immunosorbent assay; GPCR, G protein-coupled receptor; WT, wild type; IL, interleukin; GAG, glycosaminoglycan; ANOVA, analysis of variance; AM, acetoxymethyl ester; ZY, zymosan.

four families on the basis of structure—C, CC, CXC, and CX_3C (Zlotnik and Yoshie, 2000)—and viral chemokine binding proteins show differential specificity and may bind one family or multiple families. The M3 protein from murine γ-herpesvirus 68, for example, binds and inactivates all known chemokines (Parry et al., 2000).

All poxviruses, including vaccinia virus, express a soluble 35-kDa chemokine-binding protein named "35K" or vCCI (Smith et al., 1997; Alcamí et al., 1998). 35K has no sequence homology with known proteins, and the elucidation of its crystal structure showed an unusual β-sandwich topology not seen elsewhere (Carfí et al., 1999). 35K binds all known human and mouse CC chemokines with high affinity (in the low nanomolar range), and this activity contributes directly to virulence (Burns et al., 2002; Reading et al., 2003). 35K shows the highest affinity for a number of chemokines responsible for monocyte/macrophage recruitment including MCP-1 (CCL2), MIP-1α (CCL3), MIP-1β (CCL4), and RANTES (CCL5), and indeed binds these chemokines with a higher affinity than they bind their cognate receptors (Burns et al., 2002). A solution structure of 35K in complex with the chemokine MIP-1β (CCL4) demonstrated that 35K binds tightly across the face of the chemokine, obscuring regions essential for chemokine receptor binding (Zhang et al., 2006). This study and others that generated mutant CC chemokines identified key residues involved in the 35K-chemokine interaction (Beck et al., 2001; Zhang et al., 2006). The critical residues in MCP-1 required for high affinity binding to 35K were identified as Arg18, Tyr13, and Arg24—the same residues required for interaction with the MCP-1 receptor CCR2 (Beck et al., 2001). Thus, 35K may bind to chemokines in solution or bound onto the cell surface by glycosaminoglycans, thereby preventing the adhesion and directed migration of cells expressing the appropriate chemokine receptors.

35K has been shown to reduce eosinophil infiltration in a guinea pig skin model of allergic inflammation and decreased airway inflammation in a model of allergic asthma (Alcamí et al., 1998; Dabbagh et al., 2000). Both of these models are dominated by eotaxin-induced inflammatory cell recruitment, a chemokine that has moderate to low affinity for 35K compared with other CC chemokines. The highest affinity ligands for 35K are the inflammatory chemokines known to recruit monocytes in chronic inflammatory pathologies, including rheumatoid arthritis and atherosclerosis (Burns et al., 2002). Indeed, our laboratories have shown that viral delivery of 35K suppresses both diet-induced and vein graft atherosclerosis in Apoe(−/−) mice (Bursill et al., 2004, 2009; Ali et al., 2005).

Viral delivery of 35K is not ideal for several reasons, including the inflammatory response generated by the virus, the difficulty in administering a known dose, and the short-term duration of expression in the case of adenovirus (Nayak and Herzog, 2010). We therefore generated a 35K-Fc fusion protein of vaccinia virus 35K with the modified Fc domain of human IgG1. To identify amino acid residues essential for 35K activity, we performed site-directed mutagenesis of 35K-Fc and tested mutants for their ability to block chemokine effects on primary and transfected cells and in a murine model of sterile peritonitis. We generated a number of loss-of-function mutants with single amino acid substitutions and identified a residue within 35K, which, when mutated, leads to enhanced blockade of CC chemokine activity in vitro and in vivo.

Materials and Methods

Materials. All cell culture media and buffers were obtained from PAA systems (Yeovil, UK) unless otherwise specified. All laboratory chemicals were from Sigma-Aldrich (Gillingham, Dorset, UK) unless otherwise specified. PCR primers were from Eurofins MWG Biotech (London, UK), PCR reagents were from QIAGEN (Crawley, West Sussex, UK). Chemokines were purchased from Peprotech (London, UK).

Cloning and Mutagenesis of 35K-Fc. DNA encoding 35K from vaccinia virus (Lister strain) including the endogenous signal peptide was amplified from a vector containing the entire 35K gene using the following primers GCATGCTAGCATGAAACAATATATCGTC (forward) and GCCGGAATTCGACACACGCTTTGAGTTT (reverse) encoding a 5′-NheI site and a 3′-EcoRI site using the HotStar Taq PCR kit from QIAGEN according to manufacturer's instructions. 35K was cloned in frame and upstream of a human IgG1 Fc domain using the pSecTag2(C) vector (Invitrogen, Paisley, UK). The Fc portion had been mutated previously to contain the substitutions L234A, L235E, and G237A to abrogate Fc receptor binding and P331S to prevent complement activation. 35K-Fc was mutated using the Stratagene QuikChange mutagenesis kit (Agilent Technologies, Stockport, Cheshire, UK) according to manufacturer's instructions and mutants screened by sequencing in both directions. The primers used for mutagenesis are listed in Table 1. The MR-Fc construct described here is a nonfunctional mutant of the cysteine-rich domain of the mannose receptor fused to the same mutated IgG1 Fc (Taylor et al., 2004) and was a kind gift from Dr. Philip Taylor (Department of Infection, Immunity and Biochemistry, Cardiff University, Cardiff, Wales, UK).

Production of 35K-Fc Protein. Plasmid DNA was prepared using the Endofree Plasmid maxi kit (Invitrogen) and transfected into 293T cells in triple layer T175 flasks (Nalge Nunc International,

TABLE 1
Sequences of primers used for site-directed mutagenesis of 35K-Fc

Mutation	Primers
Y80A	
Forward	TGTAGATCCTCCTACCACTGCTTACTCCATCATCGGTGGA
Reverse	TCCACCGATGATGGAGTAAGCAGTGGTAGGAGGATCTACA
R89A	
Forward	CATCATCGGTGGAGGTCTGGCAATGAACTTTGGATTCACC
Reverse	GGTGAATCCAAAGTTCATTGCCAGACCTCCACCGATGATC
D141A	
Forward	CTCTTGCTATGATCAAAGCCTGTGAGGTGTCTATCGA
Reverse	TCGATAGACACCTCACAGGCTTTGATCATAGCAAGAG
D141L	
Forward	GTGAAGAAGCTCTTGCTATGATCAAACTCTGTGAGGTGTCTATC
Reverse	GATAGACACCTCACAGAGTTTGATCATAGCAAGAGCTTCTTCAC
D141R	
Forward	GTGAAGAAGCTCTTGCTATGATCAAACGCTGTGAGGTGTCTATC
Reverse	GATAGACACCTCACAGCGTTTGATCATAGCAAGAGCTTCTTCAC
E143A	
Forward	CTATGATCAAAGACTGTGCGGTGTCTATCGACATCAG
Reverse	CTGATGTCGATAGACACCGCACAGTCTTTGATCATAG
E143K	
Forward	AGCTCTTGCTATGATCAAAGACTGTAAGGTGTCTATCGA
Reverse	TCGATAGACACCTTACAGTCTTTGATCATAGCAAGAGCT
E143R	
Forward	GAAGCTCTTGCTATGATCAAAGACTGTAGGGTGTCTATCGACA
Reverse	TGTCGATAGACACCCTACAGTCTTTGATCATAGCAAGAGCTTC
V185A	
Forward	CATCGGTTCAACGATCGCCGATACAAAATGCGTCA
Reverse	TGACGCATTTTGTATCGGCGATCGTTGAACCGATG
Y217A	
Forward	AGGTCAAGGATGGATTCAAGGCTGTCGACGGATCGGC
Reverse	GCCGATCCGTCGACAGCCTTGAATCCATCCTTGACCT
Y217N	
Forward	CAAGGATGGATTCAAGAATGTCGACGGATCGGC
Reverse	GCCGATCCGTCGACATTCTTGAATCCATCCTTG

Rochester, NY) using GeneJuice transfection reagent (Merck, Nottingham, UK) according to the manufacturer's instructions. Twenty-four hours after transfection, cells were transferred to serum-free media [Dulbecco's modified Eagle's medium plus 0.1% (w/v) BSA], and protein expression continued for 5 days. Conditioned media containing 35K-Fc was concentrated using a Vivaflow 50 tangential flow machine with a 30-kDa filter (Generon, Maidenhead, Berkshire, UK) then applied to a Proteus protein A midi column (Pierce, Cramlington, Northumberland, UK). Bound protein was washed twice with PBS/0.01% Tween 20 and then eluted with 0.5 M sodium citrate pH 3 followed by neutralization with 1.5 M Tris-HCl, pH 10. Eluted protein was dialyzed twice overnight against 4 L PBS and then reconcentrated using a centrifugal concentrator with a 30-kDa cutoff (Generon). Protein yield was assessed using a NanoDrop spectrophotometer at 280 nm, protein integrity was assessed on an SDS-polyacrylamide gel electrophoresis gel, and endotoxin testing was performed using the Pyrogene recombinant factor C assay (Lonza, Slough, UK).

Bio-Gel Elicitation of Primary Mouse Macrophages. All animal studies were conducted with ethical approval from the Dunn School of Pathology Local Ethical Review Committee and in accordance with the UK Home Office regulations (Guidance on the Operation of Animals, Scientific Procedures Act, 1986). C57BL6/J or SV129 mice (Harlan Laboratories, Blackthorn Bicester, Oxfordshire, UK) were injected intraperitoneally with 1 ml of 2% Bio-Gel P-100 fine polyacrylamide beads (45–90 μm; Bio-Rad Laboratories, Hemel Hempstead, Hertfordshire, UK) suspended in PBS, and 4 days later, mice were sacrificed, and the peritoneum was lavaged with 10 ml of ice-cold PBS/2 mM EDTA (for chemotaxis and xCELLigence assays). Room temperature PBS/EDTA was used for lavage of cells for calcium flux assays.

Calcium Flux. Cells (1×10^7/ml) were loaded with Fura-PE3 AM calcium-sensitive dye (Merck) at a concentration of 1.5 μM in calcium flux buffer [Hanks' balanced salt solution/5 mM HEPES/0.5% (w/v) BSA] for 45 min at room temperature with gentle agitation. Cells were washed twice with calcium flux buffer and then resuspended at a concentration of 3×10^7 cells/ml. Calcium flux was assessed using a PerkinElmer LS55 spectrofluorometer (PerkinElmer Life and Analytical Sciences, Waltham, MA) in a cuvette containing 100 μl of cells and 300 μl of buffer. Agonists were added in a volume of 10 μl of at a concentration of 40×. When 35K-Fc was used, agonists were preincubated with 35K-Fc for 2 h at room temperature before assay.

Chemotaxis. Chemotaxis was assessed using Neuroprobe ChemoTx 96-well plates (Receptor Technologies, Leamington Spa, Warwickshire, UK) as described previously (Cash et al., 2008). Agonists were preincubated with 35K-Fc for 2 h at room temperature and loaded into the lower well of the plate. Bio-gel-elicited primary mouse macrophages were resuspended at 5×10^6 cells/ml in chemotaxis buffer [RPMI/25 mM HEPES/0.5% (w/v) BSA], and 80 μl of cell suspension (4×10^5 cells) was placed on top of a filter with an 8 μm pore size. Cells were allowed to migrate for 4 h, and then unmigrated cells on top of the filter were removed by wiping with cotton buds. Migrated cells on the underside were fixed with 1% (v/v) formalin for 10 min, stained with 4,6-diamidino-2-phenylindole for 5 min, and filters were mounted onto slides. Migrated cells were assessed by fluorescence microscopy and quantified using MetaMorph software (Molecular Devices, Sunnyvale, CA). Data are expressed as migration index (i.e., fold change over the response to media alone).

DiscoveRx PathHunter eXpress Beta Arrestin Assay. The assay was performed according to manufacturer's instructions (DiscoveRx Corporation, Birmingham, UK). In brief, cells were thawed and plated in OCC media in half area 96-well luminescence plates (white-walled, clear-bottomed) and allowed to recover for 48 h. Agonists were preincubated ± 35K-Fc for 2 h at room temperature and then added to the cells for 90 min at 37°C. Detection reagents were added and incubated with the cells for 90 min at room temperature. Luminescence was measured using a 96-well plate luminometer and WinGlow Software (Berthold Instruments, Harpenden, Hertfordshire, UK).

Roche xCELLigence Electric Cell-Substrate Impedance Sensing Assay. Experiments were performed using a 96-well xCELLigence SP instrument (Roche Diagnostics, Burgess Hill, West Sussex, UK). Bio-gel-elicited macrophages were plated at 200,000 cells/well in 96-well xCELLigence plates in Opti-MEM media (Invitrogen) and allowed to adhere for 6 h before the media were changed to remove nonadherent cells. The following day, agonists were preincubated ± 35K-Fc for 2 h at room temperature and then added to the cells, and data were collected every 2 s. The data were normalized to the addition of media alone, and then the maximum cell index (i.e., peak height) was calculated. Experiments using CCR2-transfected CHO cells were performed with 25,000 cells/well.

Zymosan Induced Peritonitis. Zymosan-induced peritonitis was performed as described previously (Cash et al., 2009). In brief, C57BL6/J mice (Harlan Laboratories) were injected intraperitoneally with 10 μg of zymosan A (Sigma-Aldrich) diluted in 0.5 ml of PBS or vehicle alone. Two hours later, mice were injected with 15 μg of 35K-Fc in 0.5 ml of PBS or vehicle alone. After a further 2 h, mice were sacrificed, and the peritoneal cavity was lavaged with 5 ml of PBS/2 mM EDTA. Peritoneal cell counts were performed using a hemocytometer and trypan blue exclusion, and peritoneal exudate cells were stained with antibodies against Ly6G (BD Biosciences, Oxford, Oxfordshire, UK) and 7/4 (AbD Serotec, Kidlington, Oxfordshire, UK) and analyzed by flow cytometry to assess neutrophil and inflammatory monocyte recruitment (see Supplementary Fig. 1 for representative primary data). Cell-free peritoneal lavage fluid was stored at −80°C for later ELISA analysis.

35K Sandwich ELISA. Maxisorb ELISA plates (Nalge Nunc International) were coated overnight at room temperature with vCCI (35K) capture antibody (R&D Systems, Minneapolis, MN) at 1 μg/ml in PBS. Plates were washed five times with distilled H_2O, and then nonspecific binding was blocked with blocking buffer (PBS/0.25% BSA/1 mM EDTA) for 2 h at room temperature. Lavage samples (undiluted) or standards were incubated on the plate for 2 h, washed off, and then incubated with anti-human Fc HRP antibody (diluted in blocking buffer 1:5000; Jackson ImmunoResearch Laboratories, West Grove, PA). The plate was incubated with substrate (Sigma Fast OPD), and then the reaction stopped with 3 M H_2SO_4. Calculated concentrations were multiplied by the lavage volume (5 ml) to obtain total micrograms of 35K-Fc per peritoneal cavity.

JE Sandwich ELISA. Peritoneal lavage samples were assayed for JE (mouse CCL2/MCP-1) concentration using a Duoset sandwich ELISA (R&D Systems) according to the manufacturer's instructions. Samples were assayed undiluted. Calculated concentrations were multiplied by the lavage volume (5 ml) to obtain the total nanograms of JE per peritoneal cavity.

Results

35K-Fc Specifically Blocks CC Chemokine-Induced Calcium Flux and Chemotaxis. Purified 35K-Fc protein was tested for its ability to block CC chemokine signaling in a calcium flux assay with stably transfected 300.19 murine B cells. 300.19 CCR2 cells showed a robust calcium flux in response to the CC chemokine MCP-1 (CCL2) but failed to respond to the CX_3C chemokine fractalkine (FK/CX_3CL1; Fig. 1A). Likewise, 300.19 CX_3CR1 cells responded to fractalkine but showed no response to MCP-1 (Fig. 1B). Both cell lines responded to SDF-1α (CXCL12) via their endogenous CXCR4 receptor (Fig. 1, A and B). MCP-1 preincubated with 35K-Fc failed to induce a calcium flux in 300.19 CCR2, and a second addition of MCP-1 also failed to induce signaling, presumably because of rapid binding and inactivation of the chemokine by 35K-Fc (Fig. 1C). SDF-1α still induced a cal-

cium signal, indicating a specific blockade of CC chemokine signaling (Fig. 1C). Furthermore, 35K-Fc had no effect on the response to the CX_3C chemokine fractalkine in 300.19 CX_3CR1 cells (Fig. 1D). A second addition of fractalkine failed to induce a calcium flux response, presumably because of homologous desensitization of the CX_3CR1 receptor (Fig. 1D).

To further confirm the specificity of the CC chemokine blockade by 35K-Fc, we performed a calcium flux assay in primary Bio-gel elicited murine macrophages. These cells showed a robust calcium flux response to the CC chemokine agonist MIP-1α (CCL3) and the nonchemokine GPCR agonist leukotriene B4 (LTB4), which acts through the BLT1 receptor (data not shown). 35K-Fc almost completely abrogated the response to MIP-1α but had no effect on the response to LTB4 (Fig. 2A). A second addition of MIP-1α alone did elicit a calcium flux, showing that the cells were capable of responding. A control Fc protein (MR-Fc: a nonfunctional fusion of the cysteine rich domain of mannose receptor with the same IgG1 Fc domain) (Taylor et al., 2004) had no effect on the macrophage response to MIP-1α, indicating that the blockade is specific to 35K-Fc (Fig. 2B). A second addition of MIP-1α failed to induce a significant calcium flux presumably because of homologous desensitization of the receptor.

We next tested whether 35K-Fc could inhibit chemotaxis of primary macrophages toward CC chemokines. Bio-gel-elicited murine macrophages were allowed to migrate toward increasing concentrations of MIP-1α and showed a bell-shaped dose-response curve, which is typical in this modified Boyden chamber assay (Fig. 2C). We then chose a fixed dose of 0.5 nM MIP-1α and preincubated the chemokine with increasing doses of 35K-Fc for 1 h before addition to the assay. 35K-Fc induced a dose-dependent blockade of MIP-1α-induced migration that was statistically significant at doses of 5, 10, and 20 nM (Fig. 2D). 35K-Fc had no effect on macrophage chemotaxis toward the potent chemoattractant chemerin (a nonchemokine) at any dose tested (data not shown).

Site-Directed Mutagenesis and Screening by PathHunter eXpress β-Arrestin GPCR Assay. Site-directed mutagenesis of MCP-1, a high-affinity ligand for 35K, indicated that the residues Tyr13, Arg18, and Arg24 in the chemokine were essential for binding to both 35K and the MCP-1 receptor CCR2 (Beck et al., 2001). These residues are highly conserved among all CC chemokines, and a solution structure of MIP-1β bound to rabbitpox 35K indicated that these same residues were closely contacted by 35K and highlighted the critical residues involved (Zhang et al., 2006). We targeted a number of residues within 35K based on the information provided by the costructure. Asp141 and Glu143 interact closely with the positively charged Arg18 residue in the chemokine, we therefore generated charge-swap mutants D141R, E143K, and E143R and alanine mutants D141A and E143A and a D141L mutant with a larger, hydrophobic, uncharged side chain. Phe13 in the chemokine was shown to contact a cluster of hydrophobic residues, including Val185 and Tyr217. We generated alanine mutants at these two residues and generated a polar Y217N mutant to disrupt the hydrophobic binding site. Finally, mutagenesis of MCP-1 by Beck et al. (2001) revealed that the mutation K49A in MCP-1

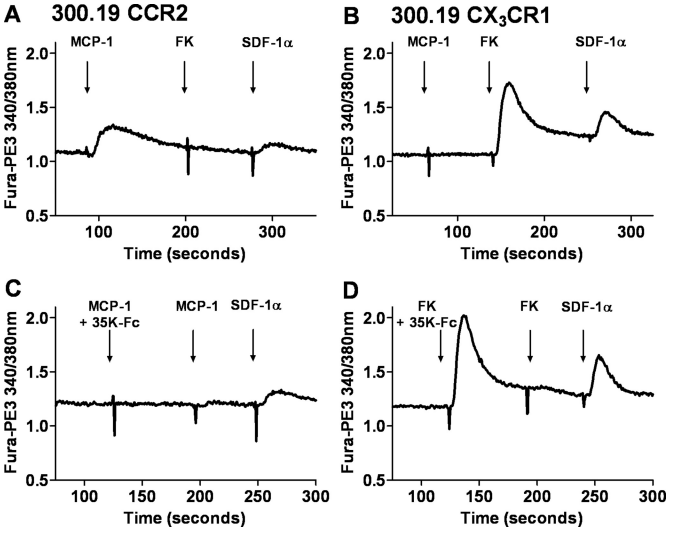

Fig. 1. 35K-Fc inhibition of chemokine-induced calcium flux in transfected cells. 300.19 cells stably transfected with CCR2 or CX_3CR1 were loaded with the ratiometric calcium sensitive dye Fura-PE3 AM and analyzed using a spectrofluorometer. Chemokines (2.5 nM) were added at the indicated time points and data collected every 0.5 s (A and B). Chemokines (2.5 nM) were preincubated with 50 nM 35K-Fc for 2 h at room temperature before addition (C and D). A to D are representative of three independent experiments, each with two technical replicates per experiment.

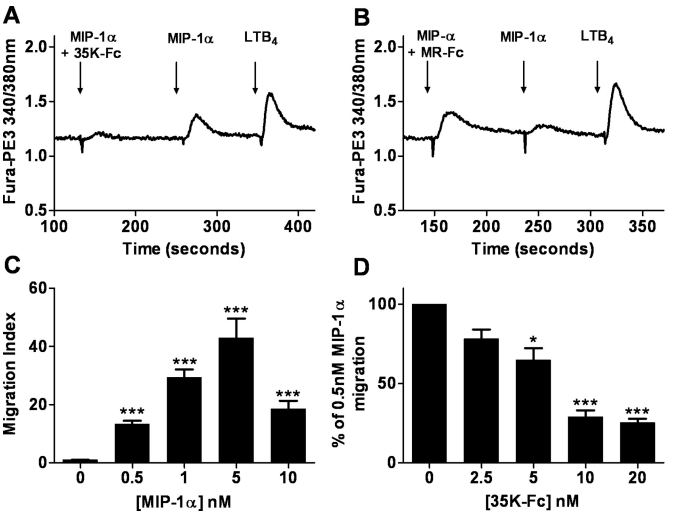

Fig. 2. 35K-Fc inhibition of chemokine-induced calcium flux and chemotaxis in primary mouse macrophages. A and B, bio-gel-elicited murine macrophages from SV129 mice were loaded with the ratiometric calcium sensitive dye Fura-PE3 AM and analyzed using a spectrofluorometer. MIP-1α (10 nM) and LTB4 (1 μM) were added at the indicated times, and data were collected every 0.5 s (A and B). MIP-1α was preincubated with 30 nM 35K-Fc (A) or MR-Fc (B) for 2 h before addition. Data are representative of three independent experiments with two technical replicates per experiment. C and D, bio-gel-elicited murine macrophages from SV129 mice in the upper chamber of a Neuroprobe ChemoTx plate were allowed to migrate toward the indicated concentration of MIP-1α for 4 h (C). Migration was assessed by staining cells on the underside of the chemotaxis filter. Data are shown as migration index (i.e., fold change over media alone) and are the mean ± S.E.M. of four to six independent experiments, each with three technical replicates per experiment. D, primary macrophages were allowed to migrate for 4 h toward MIP-1α (0.5 nM), which had been preincubated with the indicated concentration of 35K-Fc for 30 min. Data are shown as a percentage of 0.5 nM MIP-1α-induced migration, and are the mean ± S.E.M. of four independent experiments with three technical replicates per experiment. Statistical analysis performed by one-way ANOVA and Dunnett's multiple comparison post test. *, $p < 0.05$ relative to MIP-1α alone, ***, $p < 0.001$ relative to media alone (C) or MIP-1α alone (D).

increased its affinity for 35K by 3-fold, possibly by relieving steric hindrance in this region of interaction (Beck et al., 2001). In the costructure, this residue was found to be closely contacted by the residues Tyr80 and Arg89 in 35K (Zhang et al., 2006). We hypothesized that alanine mutants of these residues in 35K would show higher affinity chemokine binding than the WT protein.

Mutant 35K-Fc proteins were produced in exactly the same way as WT protein and integrity assessed by SDS-polyacrylamide gel electrophoresis gel and Western blotting with anti-35K antibody (data not shown). To screen the mutants for their effect on CC chemokine activity, we used a rapid and robust GPCR signaling assay based on β-arrestin recruitment in transfected cell lines (DiscoveRx PathHunter eXpress).

RANTES induced a dose-dependent activation of CCR5 with an EC_{50} of 2 nM (Fig. 3A). To test the effect of 35K-Fc on CCR5 activation by RANTES, 5 nM RANTES (the EC_{80} in this assay) was preincubated for 2 h with 35K-Fc at a range of concentrations and then added to the assay. WT 35K-Fc inhibited CCR5 activation and β-arrestin recruitment with an IC_{50} of 5.6 nM (Fig. 3B). MR-Fc had no effect on CCR5 activation by RANTES at any dose tested (Fig. 3B).

To screen the mutants, 5 nM RANTES was preincubated with 35K-Fc at a fixed dose (15 nM) for 2 h and then added to the assay. When RANTES was preincubated with WT 35K-Fc, the response was approximately 38% of that with RANTES alone (Fig. 3C). All other mutants, except for V185A, had a significantly different effect ($p < 0.001$) on RANTES signaling at CCR5 compared with WT 35K-Fc. Mutations at Asp141 and Glu143 significantly inhibited chemokine blockade, with the E143K and E143R charge-swap mutants showing complete (>95%) loss of function, indicating the crucial importance of contact with the Arg18 residue in the chemokine (Fig. 3C). Mutations targeting the interaction with Phe13 in the chemokine indicated that the Val185 residue in 35K is not critically involved in the interaction, whereas Tyr217 mutation does reduce the extent of chemokine blockade but this residue is not essential for function (Fig. 3C).

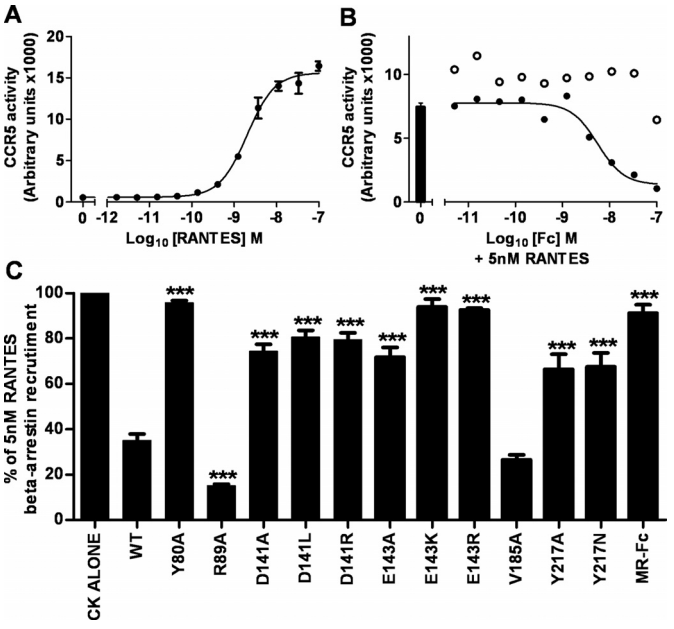

Fig. 3. Screening of 35K-Fc mutants by CCR5 DiscoveRx assay. A, dose-response curve showing recruitment of β-arrestin in response to CCR5 activation by RANTES as measured by PathHunter eXpress assay (DiscoveRx). B, RANTES (5 nM) was preincubated for 2 h with the indicated concentration of WT 35K-Fc (●) or MR-Fc (○) and then added to the assay. A and B show mean ± S.E.M. of two technical replicates and are representative of three independent experiments. C, RANTES (5 nM) was preincubated with the indicated 35K-Fc mutant (fixed dose, 15 nM) and then added to PathHunter eXpress CCR5 transfected cells and β-arrestin recruitment measured according to manufacturer's instructions. Data are shown as the percentage of the response to RANTES alone and are the mean of two independent experiments ± S.E.M., each with two technical replicates for two batches of protein (i.e., four wells per mutant per experiment). Statistical analysis performed by one-way ANOVA and Dunnett's multiple comparison post test. ***, $p < 0.001$ relative to WT 35K-Fc.

We hypothesized that the two mutants Y80A and R89A would show an increased ability to block chemokine signaling. In fact, the Y80A mutant showed complete loss of function, indicating that this residue is essential for contact with Lys49 in the chemokine. In contrast, R89A showed an enhanced blockade of RANTES signaling compared with WT 35K-Fc ($p < 0.001$), reducing the response to 18% compared with RANTES alone (Fig. 3C). The control protein, MR-Fc was completely unable to block RANTES signaling, showing the specificity of the CC chemokine blockade (Fig. 3C). We also screened selected mutants in a second signaling assay (xCELLigence) using CCR2-transfected cells, which measures the effect of chemokines on electric cell-substrate impedance sensing (see below). Data for all mutants are summarized in Table 2.

R89A Is a More Potent Inhibitor of In Vitro Chemokine Activity than WT 35K-Fc. We chose to take two mutants for further analysis in vitro: the loss-of-function mutant E143K, and the R89A mutant with enhanced inhibitory activity. In a CCR2 β-arrestin assay, WT 35K-Fc inhibited the response to MCP-1 with an IC_{50} of 12.9 nM in the experiment shown, whereas R89A 35K-Fc was significantly more potent ($p < 0.001$) and inhibited MCP-1 signaling with an IC_{50} of 2.8 nM (Fig. 4B, pooled data from independent experiments are shown in Table 2). In a CCR5 β-arrestin assay, WT 35K-Fc inhibited the response to RANTES with an IC_{50} of 7.2 nM in the experiment shown, whereas R89A 35K-Fc was again more potent ($p < 0.05$) and inhibited RANTES signaling with an IC_{50} of 2.5 nM (Fig. 4D, pooled data from independent experiments are shown in Table 2). R89A also showed a more potent blockade of the CCR7 ligand MIP-3β (CCL19; $p < 0.01$; Table 2). In contrast, E143K 35K-Fc had no effect on either MCP-1- or RANTES-induced receptor activation, indicating that it is a loss-of-function mutant (Fig. 4, B and D, and Table 2). Neither WT nor R89A 35K-Fc was able to block the activity of IL-8 (CXCL8) on the CXCR2 receptor, indicating a specific blockade of CC chemokine activity only (Fig. 4F).

To test whether the mutants showed similar activity on primary cell responses to chemokines, we used an electric cell-substrate impedance sensing (ECIS) assay (Roche xCELLigence), which measures changes in cell impedance as a result of functional responses (Yu et al., 2006). Primary bio-gel-elicited primary murine macrophages were plated in a 96-well xCELLigence plate, in which the base of the plate is covered with gold electrodes. Alternating current is passed through the cell monolayer every 2 s, and impedance is measured in an arbitrary unit termed "cell index." When

cells are stimulated with an agonist, a change in impedance occurs, which causes an increase in the cell index that can be measured over time. Representative primary data obtained by treating macrophages with either MIP-1α (CCL3) or SDF-1α (CXCL12) are shown in Fig. 5, A and B, respectively.

The chemokine MIP-1α (CCL3) induced a dose-dependent increase in cell index in primary murine macrophages with an EC_{50} of approximately 0.9 nM (Fig. 5, A and C). To test the effect of the 35K-Fc mutants on this response, 4 nM MIP-1α ($\sim EC_{80}$ of the assay) was preincubated with increasing concentrations of WT or mutant 35K-Fc for 2 h and then applied to the assay. WT 35K-Fc inhibited the response to MIP-1α with an IC_{50} of 3.6 nM in the experiment shown (Fig. 5E, pooled data from independent experiments is shown in Table 2). R89A 35K-Fc was approximately twice as potent as WT 35K-Fc ($p < 0.05$), and inhibited the response with an IC_{50} of 1.7 nM in the experiment shown (Fig. 5E; pooled data from independent experiments are shown in Table 2). E143K was completely unable to inhibit the response to MIP-1α (Fig. 5E). To confirm that R89A 35K-Fc remained a specific inhibitor of CC chemokines, we used the CXC chemokine SDF-1α in the same assay. In primary murine macrophages, SDF-1α induced an increase in cell index with an EC_{50} of approximately 4.7 nM (Fig. 5, B and D). Neither WT nor R89A 35K-Fc had any effect on the response when preincubated with SDF-1α before addition to the assay (Fig. 5F).

R89A Shows Enhanced Blockade of Monocyte Recruitment In Vivo Compared with WT 35K-Fc. To test the effect of wild-type and mutant 35K-Fc on inflammatory cell recruitment in vivo, we used a sterile model of peritonitis induced by the yeast cell wall component zymosan (Cash et al., 2009). To determine whether 35K-Fc could inhibit ongoing inflammation, mice were injected intraperitoneally with zymosan, then 2 h later were injected with wild-type or mutant 35K-Fc. A low dose of 35K-Fc was chosen (15 μg) such that potential differences in activity between mutants could be quantified. Peritoneal lavage was carried out 2 h later (after 4 h overall), and total cell counts were performed as well as staining and flow cytometry to measure neutrophil and monocyte recruitment (see Supplementary Fig. 1 for representative flow cytometry data). WT 35K-Fc (15 μg) significantly reduced monocyte recruitment by 30% (Fig. 6A; $p < 0.05$) but had no effect on neutrophil influx (Fig. 6B) or total cell numbers in the cavity (data not shown). The R89A mutant also significantly blocked monocyte recruitment into the cavity by 43% (Fig. 6A; $p < 0.001$), whereas the E143K mutant showed total loss of function and had no effect on monocyte recruitment (Fig. 6A).

We also assessed the level of the CC chemokine JE (mouse MCP-1/CCL2) in peritoneal lavage fluid from the same animals using an ELISA capable of detecting free chemokine and that bound to 35K-Fc protein. Control mice receiving vehicle alone (PBS, PBS group) had a low level of peritoneal JE (0.13 ng/cavity; Fig. 6C), and this increased 3.5-fold to 0.49 ng/cavity after the injection of zymosan (ZY, PBS group; Fig. 6C). Injection of 35K-Fc protein alone also led to an increase in the level of peritoneal JE detectable (0.63 ng/cavity; PBS, 35K group). Mice receiving zymosan followed by WT 35K-Fc (ZY, WT group) had significantly more peritoneal JE than mice receiving zymosan alone (0.78 ng/cavity; $p < 0.05$, Fig. 6C). Furthermore, injection of zymosan followed by R89A 35K-Fc further enhanced the level of detectable JE (1.1 ng/cavity; $p < 0.001$), whereas injection of the loss-of-function E143K mutant did not significantly alter the level of peritoneal JE compared with animals receiving zymosan alone (0.34 ng/cavity; Fig. 6C).

To confirm that all animals received equivalent doses of the 35K-Fc proteins, we assayed the lavage fluid with a 35K sandwich ELISA. Two hours after injection, there was approximately 1 μg of 35K-Fc remaining in the peritoneal cavity and no significant difference between treatment groups (Fig. 6D).

TABLE 2

Summary of data for 35K-Fc mutants

Values are presented as mean ± S.D. Column 2 summarizes data shown in Fig. 3C and indicates the response to 5 nM RANTES (set as 100%) in a CCR5 DiscoveRx assay after preincubation of 5 nM RANTES with 15 nM 35K-Fc. Column 3 gives the IC_{50} (mean of two technical replicates) for the indicated 35K-Fc mutant in a single xCELLigence ECIS screening assay with CCR2-transfected CHO cells responding to 10 nM MCP-1. Columns 4 to 7 show the IC_{50} from the number of independent experiments as indicated in parentheses. Statistical analysis was performed by unpaired t test. Columns 4 and 5 summarize the data shown in Fig. 4. Column 6 gives the IC_{50} for the indicated 35K-Fc mutant in a DiscoveRx assay with CCR7-transfected CHO cells responding to 10 nM MIP-3β (CCL19). Column 7 summarizes the data shown in Fig. 5. The final column indicates the overall rank of the mutants (1, most potent chemokine blockade; 11, least potent).

Mutant	RANTES Response (CCR5 DiscoveRx)	IC_{50}					Overall Rank
		CHO-CCR2 xCelligence	CCR5 DiscoveRx	CCR2 DiscoveRx	CCR7 DiscoveRx	MΦ xCelligence	
	%			*nM*			
WT	35.1	90.0	6.6 ± 0.9 (3)	13.9 ± 1 (3)	12.2 ± 0.4 (2)	3 ± 0.8 (3)	3
Y80A	95.6	>1000					10
R89A	15.1	20.6	3.7 ± 1.7 (4)*	3.1 ± 0.4 (2)***	4.1 ± 0.1 (2)**	1 ± 0.4 (3)*	1
D141A	74.3	139.0					4
D141L	80.6	>750					8
D141R	79.4	>700					6
E143A	71.7						5
E143K	93.9	>5000	N.D. (3)	N.D. (2)		N.D. (3)	11
E143R	92.5						11
V185A	26.5	50.0					2
Y217A	66.5	>5000					7
Y217N	67.5	>1400					6
MR-Fc	91.2	>1400	N.D. (3)	N.D. (2)		N.D. (3)	9

N.D., IC_{50} could not be determined (i.e., a curve could not be fitted).
* $P < 0.05$ relative to WT 35K-Fc treatment.
** $P < 0.01$ relative to WT 35K-Fc treatment.
*** $P < 0.001$ relative to WT 35K-Fc treatment.

Discussion

Using site-directed mutagenesis, this study has identified residues in a 35K-Fc fusion protein that are essential for CC chemokine binding: those that are dispensable, and others that can be mutated to enhance chemokine blockade. After the generation of a 35K-Fc fusion protein, we have shown specific and potent blockade of CC chemokine activity in vitro and demonstrated anti-inflammatory activity in vivo. Based on the published costructure between 35K and MIP-1β (Zhang et al., 2006), we produced a series of mutants targeting key residues and tested their function in vitro. With the substitution of a single residue, E143K, we generated a 35K-Fc protein that is incapable of blocking CC chemokine activity in vitro and in vivo, and we identified a residue (Arg89) that, when mutated to alanine, leads to a 35K-Fc protein with increased potency of CC chemokine blockade and enhanced anti-inflammatory activity.

The solution costructure between 35K and MIP-1β showed several key regions at the interface between 35K and the chemokine (Zhang et al., 2006). These included the acidic residues Asp141 and Glu143 and the hydrophobic pocket including the residues Val185 and Tyr217. We have demonstrated that Glu143 is the only essential residue for the electrostatic interaction with Arg18 on the chemokine, because the charge swap mutants E143K and E143R show complete loss of activity. Asp141 mutations impair the function of 35K but do not result in total loss of function. Mutation of residues in the hydrophobic pocket involved in contacting Phe13 in the chemokine revealed that the Val185 residue in 35K is not required, whereas Tyr217 is important but not essential for the interaction. Finally, experiments by Beck et al. (2001) indicated that mutation of Lys49 in MCP-1 increased the interaction with 35K . We hypothesized that mutation of the interacting residues on 35K (Tyr80 and Arg89) would increase the potency of CC chemokine blockade. In fact, Tyr80 was shown to be essential because mutation to alanine completely abrogated the function of 35K-Fc. However, the R89A mutant showed a 3- to 4-fold higher chemokine blocking activity compared with WT 35K-Fc.

In a murine model of sterile peritonitis, 35K-Fc was able to significantly reduce monocyte but not neutrophil recruitment at a relatively low dose (15 μg). The lack of effect on neutrophil recruitment is not unexpected, because the recruitment of neutrophils in this model is driven by multiple factors, including CXC chemokines and complement components (e.g., C5a). The dose used in this study is in line with clinically used Fc fusion proteins because 15 μg per mouse equates to a dose of 750 μg/kg, which, in a 70-kg adult would equate to a 50-mg injection, the recommended weekly dose for the anti-TNF Fc fusion protein etanercept. Our results

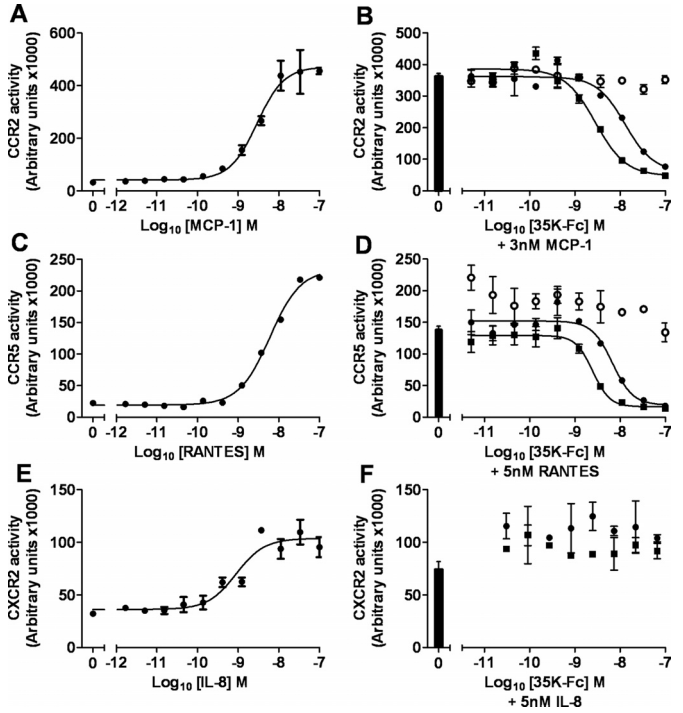

Fig. 4. Comparison of 35K-Fc WT, R89A, and E143K proteins by DiscoveRx β arrestin assay. A, dose-response curve of beta arrestin recruitment in response to CCR2 activation by MCP-1. B, MCP-1 (3 nM) was preincubated with the indicated concentration of WT 35K-Fc (●), R89A 35K-Fc (■) or E143K 35K-Fc (○) for 2 h then applied to the DiscoveRx assay. C and D, as for A and B, using CCR5 DiscoveRx cells and RANTES as the chemokine ligand. E and F, as for A and B, using CXCR2 DiscoveRx cells and IL-8 as the chemokine ligand. A and B show the mean ± S.E.M. of two technical replicates and are representative of two to three independent experiments. C and D show the mean ± S.E.M. of two technical replicates and are representative of three to four independent experiments. E and F show the mean ± S.E.M. of two technical replicates and are representative of two independent experiments.

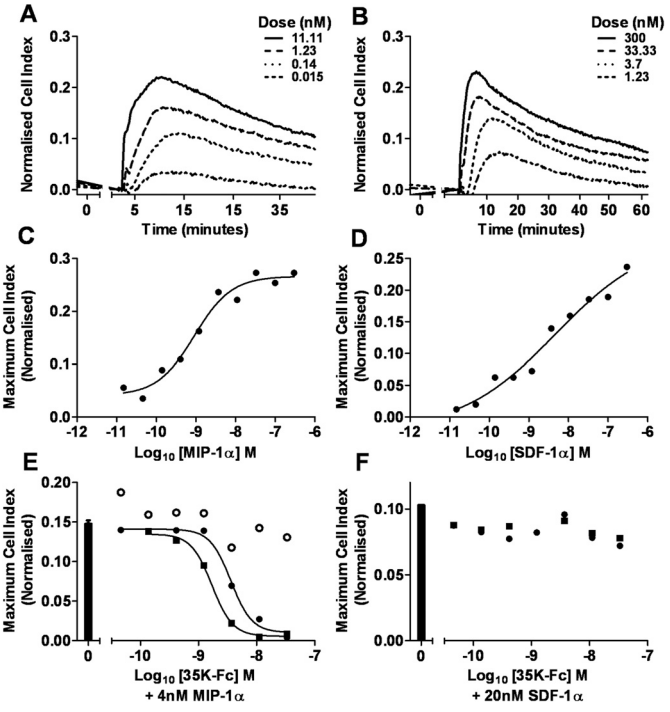

Fig. 5. Comparison of 35K-Fc WT, R89A and E143K proteins by xCELLigence assay in primary murine macrophages. Bio-gel-elicited peritoneal murine macrophages were plated in a 96-well ECIS plate (Roche xCELLigence) overnight and allowed to adhere. The next day, cells were treated with the indicated concentration of MIP-1α (A and C) or SDF-1α (B and D). Traces were normalized to wells that received vehicle alone (Opti-MEM medium) and the cell index was measured at 2-s intervals for 45 min [primary data shown for MIP-1α (A) and SDF-1α (B)]. To obtain dose-response curves, the maximum cell index (i.e., peak height) over the 45-min time course was calculated (C and D). WT (●), R89A (■), or E143K (○) 35K-Fc was preincubated with 4 nM MIP-1α (E) or SDF-1α (F) for 2 h and then applied to the assay and maximum cell index calculated as for B and D. C to F show a single technical replicate representative of three independent experiments each performed with two separate batches of each mutant protein.

also compare favorably with another study reporting the use of 35K-Fc in an air-pouch model of inflammation induced by carrageenan (Buatois et al., 2010) The authors demonstrated a 50% reduction in macrophage recruitment 72 h after a 6-h pretreatment with 200 μg of vCCi (35K)-Fc. This is approximately 13 times the dose used in our study. Furthermore, our data show that we can inhibit an ongoing inflammation induced by zymosan, a situation more relevant to inflammatory disease.

In this study, we found that although WT and R89A 35K-Fc were able to significantly reduce monocyte infiltration into the peritoneal cavity, the apparent level of the monocyte chemoattractant JE was increased. This is in line with previous studies from our laboratory, which showed that adenoviral delivery of 35K increased the plasma level of the CC chemokines RANTES and MIP-1α despite reducing the bioactivity of these chemokines (Bursill et al., 2003). We interpret this finding as evidence that 35K-Fc is able to bind and sequester chemokines in solution, preventing both their activity and clearance. Thus, the higher potency R89A mutant showed the most striking inhibition of monocyte recruitment but, on the other hand, induced the largest increase in detectable JE levels, whereas the E143K mutant neither reduced monocyte recruitment nor affected the peritoneal JE level compared with zymosan alone. This is consistent with two possible hypotheses. First, because the binding sites for 35K and glycosaminoglycans (GAGs) on chemokines are independent and differ in affinity by up to 1000-fold (35K having a low nanomolar affinity, and GAGs an approximate micromolar affinity) (Burns et al., 2002; Lau et al., 2004), 35K-Fc may "strip" chemokines bound to GAGs on the cell surface, thus increasing their apparent concentration in solution whereas disrupting chemokine gradients known to be essential for migration in vivo (Proudfoot et al., 2003). Second, binding to 35K-Fc may prevent the normal routes of chemokine clearance and degradation via decoy receptors such as D6 expressed on both lymphatic endothelial cells and recruited leukocytes (Weber et al., 2004; Graham and McKimmie, 2006; Colditz et al., 2007). D6 knockout mice show an excessive response to inflammatory stimuli, and in a cutaneous inflammation model, these mice fail to clear inflammatory chemokines in the resolution phase of inflammation, demonstrating a critical role for this receptor in chemokine clearance and degradation (Jamieson et al., 2005). Despite the fact that 35K-Fc may interfere with pathways of chemokine clearance, our results have demonstrated that 35K-Fc retains anti-inflammatory activity in vivo, suggesting that chemokines must remain bound and inactive. The pathways by which 35K-bound chemokines are cleared and degraded remain to be elucidated.

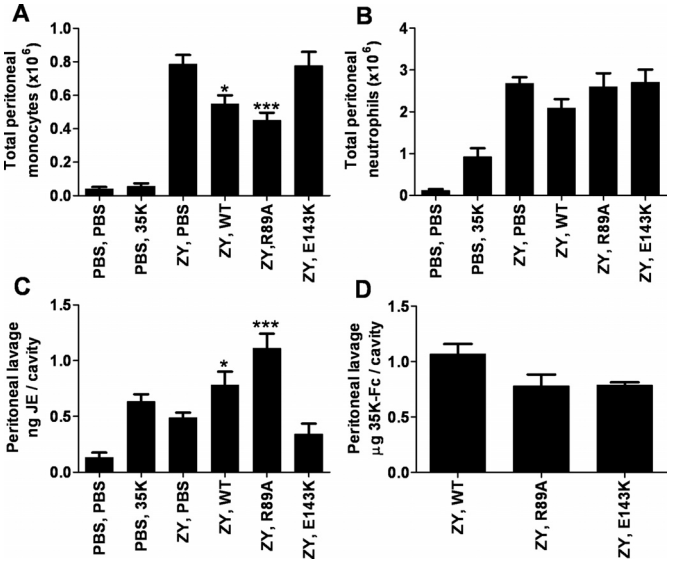

Fig. 6. Comparison of 35K-Fc WT, R89A, and E143K in a mouse model of zymosan-induced peritonitis. Mice were injected intraperitoneally with zymosan (ZY, 10 μg) or vehicle alone (PBS). Two hours later, mice were injected intraperitoneally with 15 μg of the indicated 35K-Fc protein or vehicle (PBS). After a further 2 h, mice were sacrificed, the peritoneal cavity was lavaged, and total cell counts were performed alongside fluorescence-activated cell sorting analysis for Ly6G and 7/4 to identify inflammatory monocytes (A) and neutrophils (B) (see Supplemental Fig. 1 for representative primary data). C, peritoneal lavage samples were assayed with a JE ELISA against a recombinant protein standard curve. Data are shown as nanograms of JE per cavity. D, lavage samples were assayed with a 35K-Fc sandwich ELISA and the concentration estimated against a recombinant protein standard curve. Data are shown as micrograms of 35K-Fc per cavity. Two independent experiments were performed with each mutant 35K-Fc protein, bars represent mean ± S.E.M. of 6 to 10 animals per group. Statistical analysis performed by one-way ANOVA and Dunnett's multiple comparison post test; ***, $p < 0.001$; *, $p < 0.05$ compared with zymosan, PBS group.

Fc fusion proteins and monoclonal antibodies that inhibit the activity of inflammatory mediators, including TNFα and IL-1β, are now an established therapeutic strategy in many chronic inflammatory diseases. However, not all patients respond successfully to the currently available treatment options. Chemokines may provide a novel target for therapeutic blockade in inflammatory diseases including rheumatoid arthritis, inflammatory bowel disease, and atherosclerosis, in which mouse models have shown an essential role for chemokines in pathogenesis (Boring et al., 1998; Braunersreuther et al., 2007). However, targeting a single chemokine or chemokine receptor may not prove successful because the chemokine network shows a significant level of redundancy: most chemokines bind "promiscuously" to more than one chemokine receptor, and many key chemokine receptors have multiple high-affinity chemokine ligands. Indeed, a recent study targeting a single chemokine receptor (CCR2) in atherosclerosis with a small-molecule antagonist could not halt plaque progression in experimental animals (Olzinski et al., 2010). In comparison, our laboratories have shown previously that both adenoviral and longer-term lentiviral delivery of 35K is sufficient to reduce both macrophage content and plaque size in a mouse model of atherosclerosis (Bursill et al., 2004, 2009).

In this study, we have generated a series of novel 35K-Fc fusion proteins that identify the key residues involved in CC chemokine blockade. Furthermore, we have generated a mutant protein (R89A 35K-Fc) that is more potent than the wild-type protein. These proteins should be a useful research tool to study the role of CC chemokines in pathogenesis. We believe that 35K-Fc may find therapeutic application in broad-spectrum blockade of circulating chemokines in chronic inflammatory diseases.

Acknowledgments

We acknowledge Dr. Philip Taylor (Department of Infection, Immunity and Biochemistry, Cardiff University) for the provision of the pSecTag2C vector containing the mutated IgG1 Fc domain. We thank Thomas Tan for technical assistance and advice on purifying

Fc proteins and Denise Jeffs and Linda Randall for technical support. We gratefully acknowledge funding from the British Heart Foundation Centre for Research Excellence for purchase of the Roche xCELLigence ECIS instrument.

Authorship Contributions

Participated in research design: White, McNeill, Christou, Channon, and Greaves.

Conducted experiments: White and Greaves.

Contributed new reagents or analytic tools: McNeill.

Performed data analysis: White.

Wrote or contributed to the writing of the manuscript: White, McNeill, Christou, and Greaves.

Other: Greaves and Channon acquired funding for the research.

References

Alcami A (2003) Viral mimicry of cytokines, chemokines and their receptors. *Nat Rev Immunol* **3:**36–50.

Alcamí A, Symons JA, Collins PD, Williams TJ, and Smith GL (1998) Blockade of chemokine activity by a soluble chemokine binding protein from vaccinia virus. *J Immunol* **160:**624–633.

Ali ZA, Bursill CA, Hu Y, Choudhury RP, Xu Q, Greaves DR, and Channon KM (2005) Gene transfer of a broad spectrum CC-chemokine inhibitor reduces vein graft atherosclerosis in apolipoprotein E-knockout mice. *Circulation* **112 (9 Suppl):**I235–I241.

Beck CG, Studer C, Zuber JF, Demange BJ, Manning U, and Urfer R (2001) The viral CC chemokine-binding protein vCCI inhibits monocyte chemoattractant protein-1 activity by masking its CCR2B-binding site. *J Biol Chem* **276:**43270–43276.

Boring L, Gosling J, Cleary M, and Charo IF (1998) Decreased lesion formation in CCR2(−/−) mice reveals a role for chemokines in the initiation of atherosclerosis. *Nature* **394:**894–897.

Braunersreuther V, Zernecke A, Arnaud C, Liehn EA, Steffens S, Shagdarsuren E, Bidzhekov K, Burger F, Pelli G, Luckow B, et al. (2007) Ccr5 but not Ccr1 deficiency reduces development of diet-induced atherosclerosis in mice. *Arterioscler Thromb Vasc Biol* **27:**373–379.

Buatois V, Fagète S, Magistrelli G, Chatel L, Fischer N, Kosco-Vilbois MH, and Ferlin WG (2010) Pan-CC chemokine neutralization restricts splenocyte egress and reduces inflammation in a model of arthritis. *J Immunol* **185:**2544–2554.

Burns JM, Dairaghi DJ, Deitz M, Tsang M, and Schall TJ (2002) Comprehensive mapping of poxvirus vCCI chemokine-binding protein. Expanded range of ligand interactions and unusual dissociation kinetics. *J Biol Chem* **277:**2785–2789.

Bursill CA, Cai S, Channon KM, and Greaves DR (2003) Adenoviral-mediated delivery of a viral chemokine binding protein blocks CC-chemokine activity in vitro and in vivo. *Immunobiology* **207:**187–196.

Bursill CA, Choudhury RP, Ali Z, Greaves DR, and Channon KM (2004) Broad-spectrum CC-chemokine blockade by gene transfer inhibits macrophage recruitment and atherosclerotic plaque formation in apolipoprotein E-knockout mice. *Circulation* **110:**2460–2466.

Bursill CA, McNeill E, Wang L, Hibbitt OC, Wade-Martins R, Paterson DJ, Greaves DR, and Channon KM (2009) Lentiviral gene transfer to reduce atherosclerosis progression by long-term CC-chemokine inhibition. *Gene Ther* **16:**93–102.

Carfí A, Smith CA, Smolak PJ, McGrew J, and Wiley DC (1999) Structure of a soluble secreted chemokine inhibitor vCCI (p35) from cowpox virus. *Proc Natl Acad Sci USA* **96:**12379–12383.

Cash JL, Hart R, Russ A, Dixon JP, Colledge WH, Doran J, Hendrick AG, Carlton MB, and Greaves DR (2008) Synthetic chemerin-derived peptides suppress inflammation through ChemR23. *J Exp Med* **205:**767–775.

Cash JL, White GE, and Greaves DR (2009) Chapter 17. Zymosan-induced peritonitis as a simple experimental system for the study of inflammation. *Methods Enzymol* **461:**379–396.

Charo IF and Ransohoff RM (2006) The many roles of chemokines and chemokine receptors in inflammation. *N Engl J Med* **354:**610–621.

Colditz IG, Schneider MA, Pruenster M, and Rot A (2007) Chemokines at large: in-vivo mechanisms of their transport, presentation and clearance. *Thromb Haemost* **97:**688–693.

Dabbagh K, Xiao Y, Smith C, Stepick-Biek P, Kim SG, Lamm WJ, Liggitt DH, and Lewis DB (2000) Local blockade of allergic airway hyperreactivity and inflammation by the poxvirus-derived pan-CC-chemokine inhibitor vCCI. *J Immunol* **165:**3418–3422.

Graham GJ and McKimmie CS (2006) Chemokine scavenging by D6: a movable feast? *Trends Immunol* **27:**381–386.

Jamieson T, Cook DN, Nibbs RJ, Rot A, Nixon C, McLean P, Alcami A, Lira SA, Wiekowski M, and Graham GJ (2005) The chemokine receptor D6 limits the inflammatory response in vivo. *Nat Immunol* **6:**403–411.

Lau EK, Paavola CD, Johnson Z, Gaudry JP, Geretti E, Borlat F, Kungl AJ, Proudfoot AE, and Handel TM (2004) Identification of the glycosaminoglycan binding site of the CC chemokine, MCP-1: implications for structure and function in vivo. *J Biol Chem* **279:**22294–22305.

Mackay CR (2001) Chemokines: immunology's high impact factors. *Nat Immunol* **2:**95–101.

Moreland LW, Baumgartner SW, Schiff MH, Tindall EA, Fleischmann RM, Weaver AL, Ettlinger RE, Cohen S, Koopman WJ, Mohler K, et al. (1997) Treatment of rheumatoid arthritis with a recombinant human tumor necrosis factor receptor (p75)-Fc fusion protein. *N Engl J Med* **337:**141–147.

Moreland LW, Margolies G, Heck LW Jr, Saway A, Blosch C, Hanna R, and Koopman WJ (1996) Recombinant soluble tumor necrosis factor receptor (p80) fusion protein: toxicity and dose finding trial in refractory rheumatoid arthritis. *J Rheumatol* **23:**1849–1855.

Nayak S and Herzog RW (2010) Progress and prospects: immune responses to viral vectors. *Gene Ther* **17:**295–304.

Olzinski AR, Turner GH, Bernard RE, Karr H, Cornejo CA, Aravindhan K, Hoang B, Ringenberg MA, Qin P, Goodman KB, et al. (2010) Pharmacological inhibition of C-C chemokine receptor 2 decreases macrophage infiltration in the aortic root of the human C-C chemokine receptor 2/apolipoprotein E−/− mouse: magnetic resonance imaging assessment. *Arterioscler Thromb Vasc Biol* **30:**253–259.

Parry CM, Simas JP, Smith VP, Stewart CA, Minson AC, Efstathiou S, and Alcami A (2000) A broad spectrum secreted chemokine binding protein encoded by a herpesvirus. *J Exp Med* **191:**573–578.

Proudfoot AE, Handel TM, Johnson Z, Lau EK, LiWang P, Clark-Lewis I, Borlat F, Wells TN, and Kosco-Vilbois MH (2003) Glycosaminoglycan binding and oligomerization are essential for the in vivo activity of certain chemokines. *Proc Natl Acad Sci USA* **100:**1885–1890.

Reading PC, Symons JA, and Smith GL (2003) A soluble chemokine-binding protein from vaccinia virus reduces virus virulence and the inflammatory response to infection. *J Immunol* **170:**1435–1442.

Smith CA, Smith TD, Smolak PJ, Friend D, Hagen H, Gerhart M, Park L, Pickup DJ, Torrance D, Mohler K, et al. (1997) Poxvirus genomes encode a secreted, soluble protein that preferentially inhibits beta chemokine activity yet lacks sequence homology to known chemokine receptors. *Virology* **236:**316–327.

Taylor PC and Feldmann M (2009) Anti-TNF biologic agents: still the therapy of choice for rheumatoid arthritis. *Nat Rev Rheumatol* **5:**578–582.

Taylor PR, Zamze S, Stillion RJ, Wong SY, Gordon S, and Martinez-Pomares L (2004) Development of a specific system for targeting protein to metallophilic macrophages. *Proc Natl Acad Sci USA* **101:**1963–1968.

Weber M, Blair E, Simpson CV, O'Hara M, Blackburn PE, Rot A, Graham GJ, and Nibbs RJ (2004) The chemokine receptor D6 constitutively traffics to and from the cell surface to internalize and degrade chemokines. *Mol Biol Cell* **15:**2492–2508.

Yu N, Atienza JM, Bernard J, Blanc S, Zhu J, Wang X, Xu X, and Abassi YA (2006) Real-time monitoring of morphological changes in living cells by electronic cell sensor arrays: an approach to study G protein-coupled receptors. *Analytical Chemistry* **78:**35–43.

Zhang L, Derider M, McCornack MA, Jao SC, Isern N, Ness T, Moyer R, and LiWang PJ (2006) Solution structure of the complex between poxvirus-encoded CC chemokine inhibitor vCCI and human MIP-1beta. *Proc Natl Acad Sci USA* **103:**13985–13990.

Zlotnik A and Yoshie O (2000) Chemokines: a new classification system and their role in immunity. *Immunity* **12:**121–127.

Address correspondence to: Dr. David R. Greaves, Sir William Dunn School of Pathology, University of Oxford, South Parks Road, Oxford, OX1 3RE. E-mail: david.greaves@path.ox.ac.uk